Journal of Mining and Environment (JME) Vol. 15, No. 4, 2024, 1241-1254

Shahrood University of Technology

Journal of Mining and Environment (JME)

Journal homepage: www.jme.shahroodut.ac.ir

Iranian Society of Mining Engineering (IRSME)

Exploring Ground Behavior in Underground Excavations Under Squeezing Stress Conditions

Naeem Abbas*[1,2], and Ke-gang Li[1]

1. Faculty of Land Resources Engineering, Kunming University of Science and Technology, Yunnan, China
2. Department of Mining Engineering Karakoram International University (KIU), Gilgit, Pakistan

Article Info

Received 15 February 2024
Received in Revised form 3 March 2024
Accepted 10 April 2024
Published online 10 April 2024

DOI: 10.22044/jme.2024.14198.2644

Keywords

Ground reaction curve
Numerical modeling
Support pressure
Tunneling

Abstract

The study examined the influence of cohesion, friction angle, and tunnel diameter on stability within engineering and geotechnical frameworks, while considering the consequences of nearby excavations on the overall stability assessment. The results show that a higher angle of internal friction leads to a decrease in soil stability number and weighting coefficient. Tunnel diameter significantly affects face support pressure, with larger diameters requiring stronger support due to increased stress. Higher friction angles help stabilize tunnel faces and mitigate diameter-related pressure effects. Stress redistribution around the tunnel is significant within 2 meters from the center, transitioning to elastic behavior elsewhere. A safety factor of 1.3 ensures tensile failure prevention in single and twin tunnels. Balanced stress distribution between tunnels with a slight difference is observed under isotropic in-situ stress. Numerical modeling enhances stress estimations and reveals changes during tunnel excavation, weakening the rock mass. Ground reaction curve analysis with support measures shows reduced tunnel convergence after implementation, suggesting support strategies like extended bolts using updated rock mass rating. The study improves tunnel design and stability assessment by comprehensively understanding stress redistribution and support strategies.

1. Introduction

In current times, tunnels are being built to facilitate the transportation of metros, railways, and river crossings. However, the convergence of these new construction projects with existing underground excavations has raised considerable safety concerns [1, 2]. The stress and displacement on the pre-existing tunnels are prominent as a result of building new tunnels in close or above the original tunnel [3]. A study has been conducted to examine the effects of excavating the newly created tunnel on the existing tunnel, revealing a gradual increase in stress levels due to the proximity of underground activities [4, 5]. Evaluating the impact of tunnel displacement has become progressively more significant in assessing the potential risks associated with excavations [6]. Many scholars have investigated the tunnel displacement caused by adjacent excavations [7]. Particularly, Dolezalova conducted an analysis focusing on the consequences of a deep open excavation for an office block situated above an underlying tunnel. This investigation was conducted using a 2D finite element method to comprehensively understand these effects [8]. Sharma also contributed to this field with a study that involved utilizing a finite element program to model excavation processes for tunneling [9]. Hu also studied the finite element method to conduct a thorough analysis of the displacement of a Shanghai Metro tunnel resulting from a deep excavation [10].

Numerical simulations have been utilized to model the interaction behavior between the twin tunnels [11, 12] and analytical assessment was also carried out [13] to incorporate the ground behavior for safety measures in tunneling [2, 14]. Various

Corresponding author: naeem.abbas@kiu.edu.pk (N. Abbas)

semi-empirical and analytical approaches have also been employed to rapidly predict the stability of twin tunnels [15]. While the numerical method proves influential in simulating tunnel-soil interaction in complex field conditions and during excavation procedures, it does come with the challenge of requiring a significant number of hypothetical parameters to be defined for the analysis. This can make it less convenient for real time excavations aiming to quickly predict tunnel displacement.

The stability of underground excavations is influenced by factors such as their shape, opening size, in-situ stress, and soil conditions. While the specific shape of the excavation may be considered by its intended purpose, ensuring its safe design and construction necessitates a deep understanding of stress distribution and the displacements that occur within and around the excavation [16]. When an opening is excavated within a medium, the existing in-situ stress field is disrupted, leading to the emergence of a new set of stresses induced in the surrounding area of the opening (as illustrated in Figure 1b). Understanding the magnitudes and directions of both the initial in-situ stresses and the newly induced stresses is a key element in the overall assessment and management of underground excavations [17].

As instances of these occurrences rise more frequently, the capacity to anticipate tunnel displacements has become gradually dynamic. This is particularly important for mitigating excavation risks, especially when dealing with tunnels situated above operational ones. Various practices have been developed to predict the displacements caused by adjacent excavations on tunnels. In the North Pakistan, a significant construction project involving roadworks for heavy traffic has been executed directly above an existing tunnel. In addition, this parallel tunnel has been excavated adjacent to the existing one. This situation becomes even more complex due to the highly squeezing and jointed rock mass under the influence of high stresses of the Himalayas. Furthermore, the region was tectonically active, as evidenced by the presence of significant geological features such as the main Karakoram thrust and main mantle thrust located in close proximity to this section. There are limited studies related to tunnel stability in such a complex situation. To address this challenge, three distinct approaches have been employed to assess ground reactions in this situation: analytical, approximate, and numerical methods. Each of these methods offers a unique perspective on how the ground responds to the complexities of the condition.

2. Tunnel geometry and discontinuities

The stability of tunnels was analyzed by approximate analyses as well as by numerical modeling. The approximate analysis required the results of in-situ stresses. In order to study the effect of surrounding environment on two openings, Kirsch solution has been used. The geometry of twin tunnels is shown in Figure 1a and Figure1b. The stresses around the excavations are the result from a combination of a vertical in-situ stress (σ_v), a horizontal in-situ stress (σ_h) in a plane perpendicular to the tunnel axis, and a horizontal in-situ stress (σ_{h2}) parallel to the tunnel axis. Understanding these stress distributions is essential for assessing the stability and behavior of the rock surrounding the tunnel. The properties of rocks along the tunnel route are given in Table 1. Figure 2 depicts the scenario of discontinuities, revealing the presence of multiple joints in the tunnel face. These joints exhibit varying dip angles and extend to the tunnel crown, suggesting a highly jointed rock mass. The observation of discontinuities spanning the entire distance to the tunnel crown underscores the significant challenges associated with tunneling in such rock formations.

In the face of several joints with diverse dip angles, navigating through the tunnel becomes extremely challenging. The extent of jointing in the rock mass poses additional difficulties, requiring careful consideration of engineering and excavation techniques. Understanding the nature of these discontinuities is also important for developing effective strategies to mitigate risks associated with tunnel construction in this complex geological setting. The highly jointed nature of the rock mass in the Himalayas, as illustrated in Figure 2, emphasizes the importance of comprehensive geological assessments and precise engineering solutions in order to ensure the safety and success of tunneling endeavors in this challenging environment.

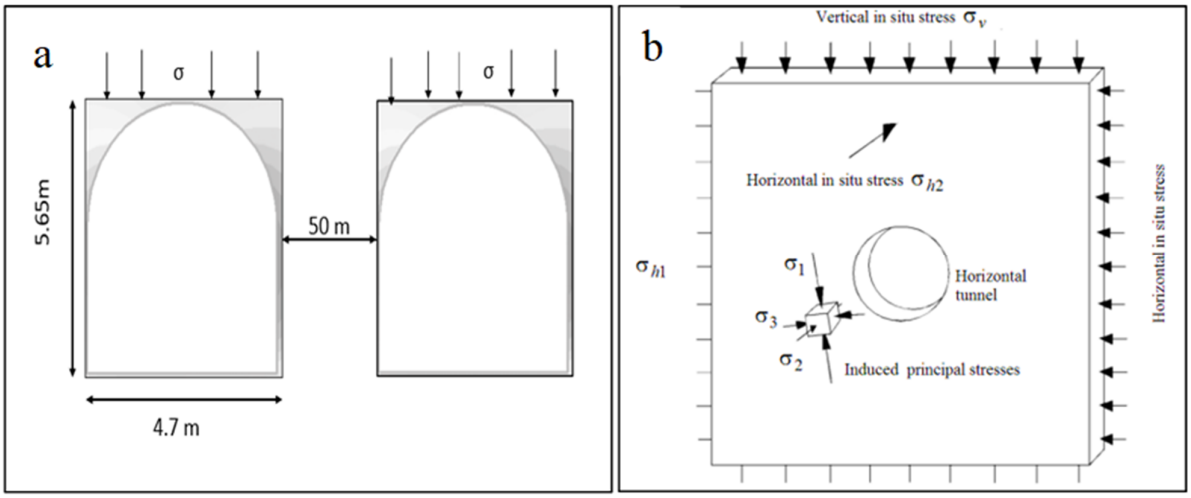

Figure 1. (a) Geometry of the tunnels (b) Influence of in-situ stresses

Figure 2. Scenario of discontinuities in Tunnel face

Table 1. Rock properties and Hoek-Brown constants.

Properties	Values
Unconfined compressive strength	80MPa
Poisson's ratio	0.249
Specific gravity	2.94
Youngs modulus	30GPa
m_b	7.98
s	0.05
a	0.5
Tensile strength	7.98MPa

The Ground Reaction Curve (GRC) has been explained incorporating rock support measures. In Figure 3a, the GRC is depicted without the implementation of support, resulting in a tunnel convergence of 0.03%. The deterministic analysis utilized the Duncan Fama solution[18]. As depicted from Figure 3b, a comparatively reduced convergence in the GRC is evident following the installation of support. To achieve the impact of ground reaction, strategies such as extending bolt length or employing the updated Rock Mass Rating, represented as RMR_{14}, for support selection have been proposed. Particularly, the influence of the ground due to the presence of the second tunnel is apparent in the approximate analysis.

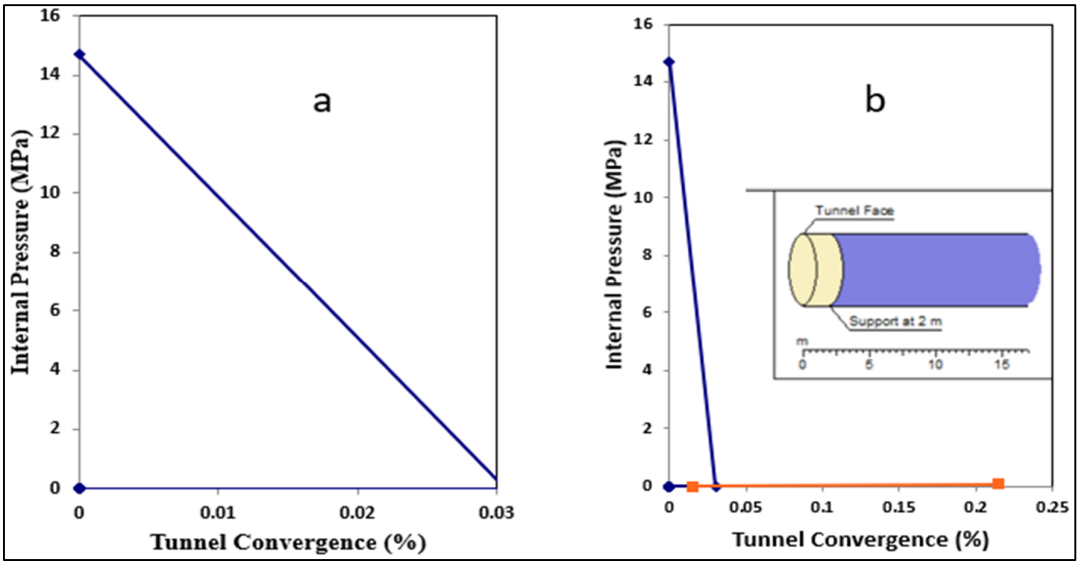

Figure 3. ground reaction curve (a) before installing support (b) after installing support

3. Approximate analysis

The Kirsch stress solution has been traditionally employed as an initial method for evaluating tunnel stability [19]. When examining the uniaxial stress state, no support pressure or internal pressure is considered. In such cases,

$$\sigma_\theta = \sigma_r = 0$$

And

$$\sigma_1 = \sigma_\theta$$

The Kirsch solution for the circumferential stress (also known as the hoop stress) around a circular opening, is given by the following expression:

$$\sigma_\theta = \frac{1}{2}\sigma_v\left[(1+k)\left(1+\frac{a^2}{r^2}\right)+(1-k)\left(1+3\frac{a^4}{r^4}\right)cos2\theta\right]$$

and for a location on the opening boundary, where a = r, this reduces to,

$$\sigma_\theta = \sigma_v\,[(1+k)+2(1-k)\cos2\theta]$$

The vertical stress is caused by the weight of the overburden, in which case we have,

$$\sigma_v = \gamma.z$$

$$\sigma_v = 0.0294 \times 500 = 14.7\ \text{MPa}$$

The stress induced at the crown and invert of the second opening, which is driven at a distance of 50m from the first opening, can be estimated using a multiple application of the Kirsch solution. The influence of one opening on another depends on the stress distribution and the interaction between the two openings.

For the crown of the second excavation/opening, we use θ = 90° in the Kirsch solution, assuming that the principal stresses align with the in-situ stress conditions from the first excavation. Using K = 1 (a coefficient associated with the Kirsch solution for a circular opening in an infinite medium) and the provided stress value of 29.4 MPa, we can calculate the additional stress induced at the crown. For the invert of the second excavation, again θ = 90° in the Kirsch solution. The stress induced at the invert would be calculated similarly to that at the crown. This approach provides an approximate solution to estimate the stress induced by the first opening on the crown and invert of the second opening, given the distance between the openings and the initial stress value

$$\sigma_\theta = \sigma_v\,[(1+k)+2(1-k)\,cos2\theta]$$

$$\sigma_\theta = 14.7\,[(1+0.2)+2(1-0.2)\,cos2*90]$$

$$\sigma_\theta = 5.88MPa$$

The stress induced in the side wall is

$$\sigma_\theta = \sigma_v\,[(1+k)+2(1-k)\,cos2\theta]$$

$$\sigma_\theta = 14.7\,[(1+0.2)+2(1-0.2)\,cos0]$$

$$\sigma_\theta = 41.16MPa$$

When the two openings are excavated, the scenario of stresses between them is calculated as, in this case r = 8.14m, and, a = 4.7m.

$$\sigma_\theta = \frac{1}{2}\sigma_v\left[(1+k)\left(1+\frac{a^2}{r^2}\right)+(1-k)\left(1+3\frac{a^4}{r^4}\right)cos2\theta\right]$$

$$\sigma_\theta = \frac{1}{2}\sigma_v\left[(1+1)\left(1+\frac{4.7^2}{8.14^2}\right)\right]$$

$\sigma_\theta = 19.6MPa$

And

$$\sigma_r = \frac{1}{2}\sigma_v\left[(1+k)\left(1-\frac{a^2}{r^2}\right)-(1-k)\left(1-3\frac{a^4}{r^4}\right)cos2\theta\right]$$

$$\sigma_\theta = \frac{1}{2}\sigma_v\left[(1+1)\left(1-\frac{4.7^2}{8.14^2}\right)\right]$$

$\sigma_\theta = 9.84MPa$

The isotropic in-situ stress implies that the stress between the two openings due to the right-hand opening and the left-hand opening is nearly the same, with a difference of 10 MPa. This indicates a relatively balanced stress distribution between the openings in this simplified scenario. To validate the accuracy of the approximate method used for estimating stress (as described in the previous response), a more realistic approach was undertaken using numerical modeling. Computational methods, such as numerical simulations, are employed to provide a more detailed and precise understanding of the stress distribution and interaction between the tunnels [20]. This modeling allows for a more comprehensive analysis, taking into account the specific geological conditions, excavation procedures, and other relevant factors [21]. The comparison between the results obtained from the approximate method and the computational method serves as a crucial check to ensure the reliability and accuracy of the approximate approach. It is important to note that while the approximate method may provide useful initial perceptions, the computational method offers a more accurate and detailed understanding of the stress behavior in the real-world scenario, taking into consideration the complexities involved [22].

4. The numerical approach

In both scenarios, the original Hoek-Brown criterion was employed to evaluate tunnel stability. The relation of rock mass quality and Hoek-Brown constant is given in Table 2. In the absence of the second tunnel's influence, the vertical stress distribution is evident: 23MPa across the crown and 14MPa alongside the walls, as demonstrated in Figure 4a. Conversely, Figure 4b displays a distinct distribution with the presence of the second tunnel, indicating vertical stress values of 25MPa around the crown and 16MPa alongside the walls.

Table 1. Relation between rock mass quality and Hoek-Brown constants [23].

Hoek-Brown Failure Criterion	s	Carbonates	Lithified argillaceous	Arenaceous	Fine-grained polymineralic igneous	Coarse-grained polymineralic igneous and metamorphic
Intact rock material	1	7	10	15	17.0	25.0
Very good rock	0.1	3.5	5	7.5	8.5	12.5
Good rock mass	0.004	0.7	1	1.5	1.7	2.5
Fair rock mass	0.0001	0.14	0.20	0.30	0.34	0.50
Poor rock mass	0.00001	0.04	0.05	0.08	0.09	0.13
Very rock mass	0	0.007	0.01	0.015	0.017	0.025

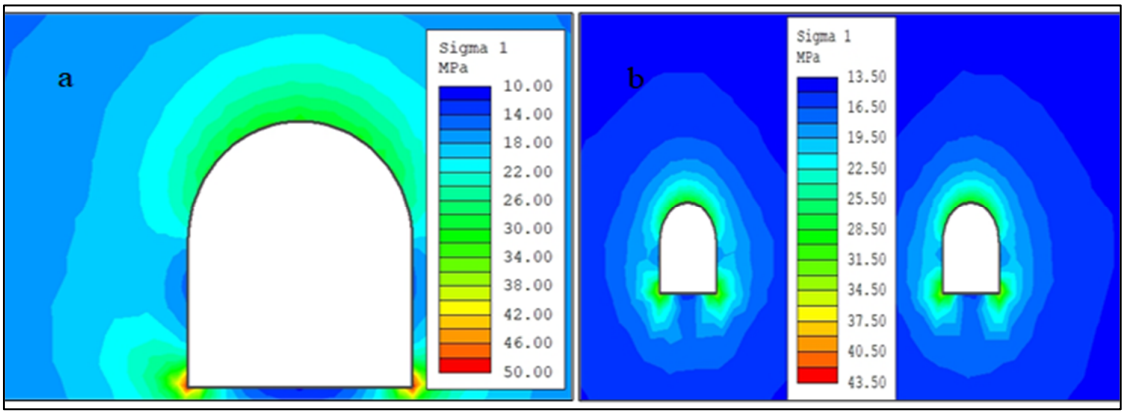

Figure 4. Major principal stress around the excavations

During the excavation of the second tunnel, there are obvious changes in the stress distribution within the stratum. This leads to a sudden stress relief in the vicinity of the excavation face. The principal stress near the main tunnel experiences a slight decrease, while the stratum far away from the excavation surface remains less disturbed [24]. Additionally, continuous tunneling of the second tunnel results in secondary ground disturbances, leading to a gradual release of stress in the area

between the twin tunnels [25]. This phenomenon progressively reduces the strength and stability of the surrounding rock mass, as observed from the contours in the Figure 4a and Figure 4b. The excavation process of the second tunnel results in a sudden stress relief around the excavation face [26]. This is a common phenomenon in tunneling, where the initial removal of rock mass reduces the confinement. The principal stress near the main tunnel experiences a slight decrease [27]. This could be due to the redistribution of stresses as the material adjacent to the main tunnel is affected by the excavation process of the second tunnel stress redistribution. The stratum far away from the excavation surface remains less disturbed. This indicates that the influence of the second tunnel excavation on the more distant rock mass is relatively limited [28]. The continuous tunneling of the second tunnel results in secondary ground disturbances. This is likely due to the interaction between the excavation processes of the two tunnels. This secondary disturbance leads to a gradual release of stress in the area between the twin tunnels. Over time, this stress release can weaken the rock mass and affect its stability [29].

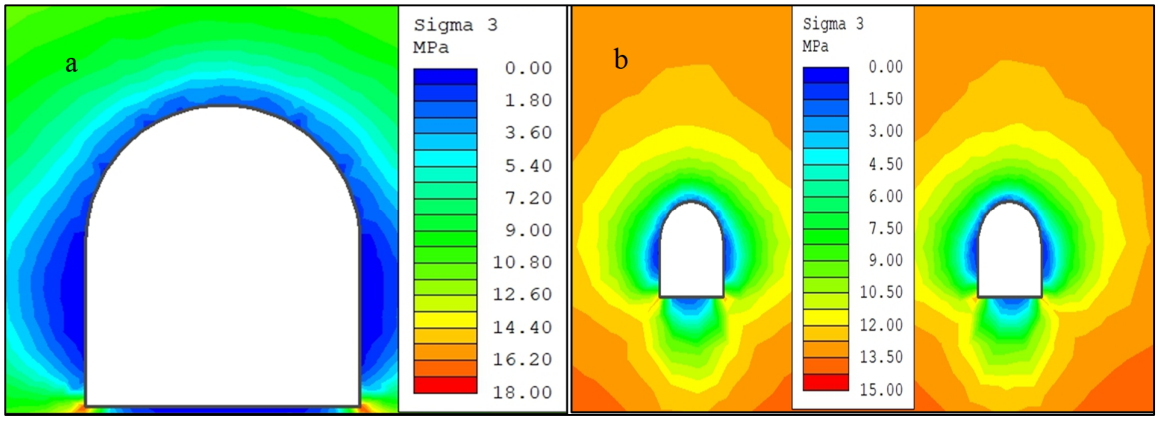

Figure 5. Minor principal stresses around the excavations.

The minor principal stress for the twin tunnel is significantly higher compared to the single tunnel. In the twin tunnel, the stress is 7.5 MPa (Figure 5b) along both the crown and the side walls, which is much higher than the single tunnel case (Figure 5a). This suggests that the presence of the second tunnel leads to higher stress levels. In the single tunnel scenario, there is a visible asymmetry in the stress distribution. This could be due to various factors, such as the geometry of the tunnel, the nature of the surrounding rock, or the stress-relief effects that occur during tunnel excavation [30]. The presence of the second tunnel has influenced the stress distribution to become more symmetrical. This could also be due to the stress redistribution effects, where the excavation of the second tunnel has equalized the stress distribution around the twin tunnels [31].

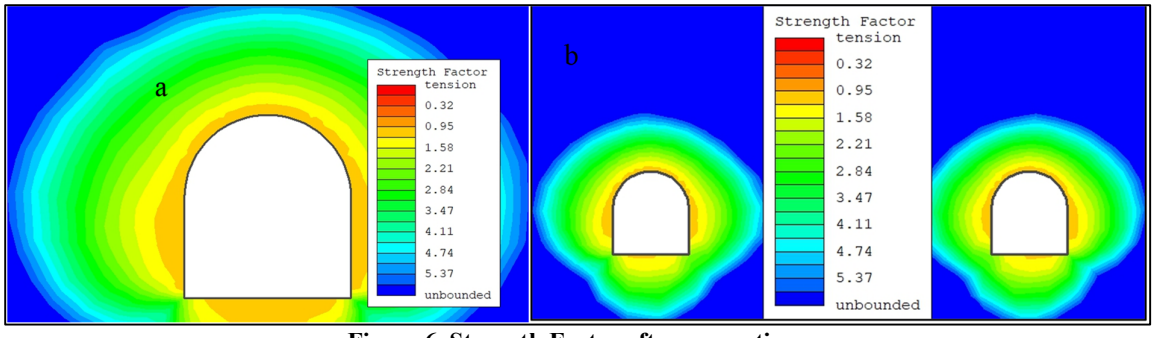

Figure 6. Strength Factor after excavations

A strength factor of 1.3 (Figure 6a and Figure 6b) in tension implies that the material around the tunnel has a factor of safety of 1.3 against tension failure. This could relate to the tensile strength of the rock mass or the ability of the surrounding material to resist tension forces. In practical terms, a factor of safety greater than 1 indicates that the material has a certain margin of safety against

failing in tension. The strength factor of 1.3 is the same for both the single tunnel and the twin tunnels. To assess the impact of tunnel geometry on the behavior of surrounding rock or soil in the section below, the effects of soil parameters, tunnel diameter, tunnel circumference, and the influence of cohesion while incorporating the angle of internal friction are investigated.

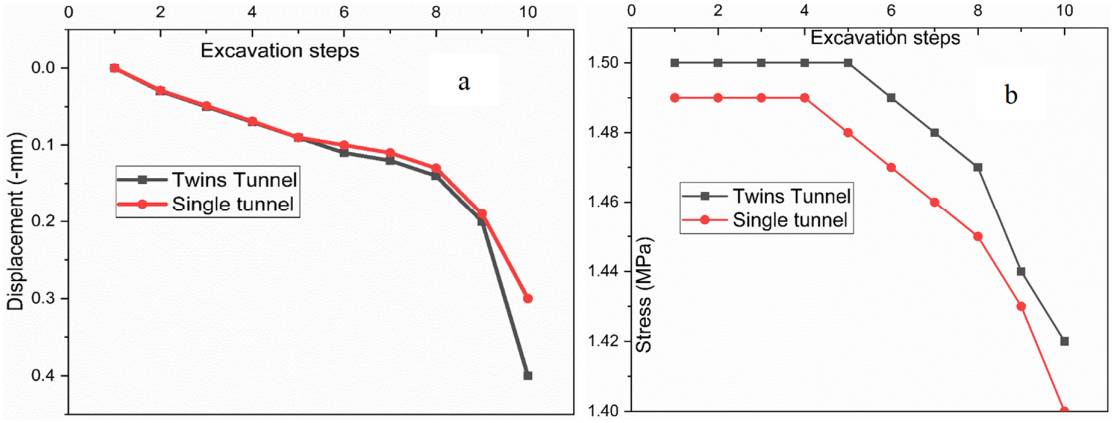

Figure 7. (a) Total displacement and (b) vertical stress distribution across both of the excavations

After analyzing the displacement changes in Figure 7a, it is evident that vertical settlement is more pronounced. The additional displacement resulting from the excavation of the second tunnel, while not as significant, suggests a relatively smaller impact. However, it is crucial to recognize that the excavation of the second tunnel continues to compromise the stability of the stratum around the openings of the twin tunnels, thereby elevating the construction risk. The normalized vertical stress (stress/in-situ stress) along the horizontal direction is depicted in Figure 7b. This clearly illustrates that the impact of vertical stress on the twin tunnels is more substantial compared to the single tunnel. An important observation is the accumulation of stress in proximity to the tunnel openings. The stress curve displays characteristics indicative of the elastic behavior of the rock mass [32].

Figure 8 illustrates the change in normalized mean stress (stress relative to in-situ stress) along the horizontal direction starting from the face of the tunnels. This plot highlights that the redistribution of stresses is concentrated in proximity to the tunnel, and at a distance of approximately 2 meters from the tunnel's center, the impact on the original in-situ stress field becomes negligible. Especially, there is a peak stress point, beyond which the material's behavior shifts from plastic to elastic. For the single tunnel, the peak stress demonstrates the plastic nature of the rock mass, signifying that the material experienced deformation beyond its elastic limit. However, after reaching this peak point, the material starts displaying elastic behavior, suggesting that it returns to its original shape when the stress is relieved. The result suggests that the stress redistribution around the tunnel has a limited influence on the far-field in-situ stress, and the overall behavior appears to be primarily elastic beyond the peak stress [32]. This is helpful for understanding the mechanical response of the rock mass to tunneling activities and aids in assessing the stability and long-term behavior of the tunnels and the surrounding ground [33].

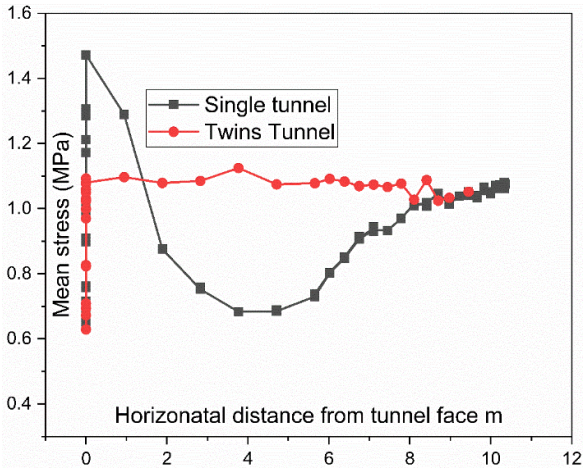

Figure 8. Variation of mean stress along the horizontal direction.

The concentration of stress redistribution in proximity to the tunnel face suggests that the immediate effects of tunneling activities are localized. This spatial confinement aligns with efficient engineering practices, as it indicates that the direct impact on the surrounding ground is

limited to a specific radius around the excavation [20]. The distinct peak stress point, indicative of plastic behavior near the tunnel face, underscores the importance of understanding the material's deformation limits during tunneling. Furthermore, the material's subsequent shift to elastic behavior beyond the peak stress implies a capacity for self-restoration, contributing to the overall resilience of the rock mass. The limited influence on far-field in-situ stress highlights the stability of the surrounding ground, affirming the reliability of the tunneling process and its minimal long-term impact on the broader geological context [34].

5. The face support pressure

The tunnel excavation diameter (D) has effect on face support pressures (P_f) [35]. The influence of tunnel diameter on face support pressure is graphically represented in Figure 9a. The tunnel diameter plays a significant role in determining the face support pressure [36]. Specifically, as the tunnel diameter increases, the limiting support pressure also increases, which suggests a clear correlation. However, it is important that the effect of diameter is mitigated when the friction angle is increased. The observed trend in Figure 9a, with increasing diameter leading to higher face support pressure. Larger tunnels require more strong support to respond to the increased stresses imposed by the larger opening. Similarly, increasing the friction angle, which is a measure of the material's resistance to sliding, helps to stabilize the tunnel face, reducing the impact of the diameter on support pressure [37].

In practical terms, understanding the relationship between tunnel diameter, friction angle, and support pressure is crucial for designing safe and stable tunnels. It is important to optimize the design of support systems based on the specific conditions of the study area, ensuring the long-term safety and functionality of the tunnels [38].

Leca et al. [39] defined the normalized face collapse pressure ($P_f/ \gamma D$) as the weighting coefficient Nγ, which can also be referred as the soil stability number or $N\gamma = Pf/ \gamma D$ in a purely frictional soil.

$$Pf = \gamma D N\gamma \quad (1)$$

The soil stability number (Nγ) can also be defined as [35],

$$N\gamma = \frac{1}{8\sin\varphi} - 0.12 \quad (2)$$

By incorporating the soil stability number, the collapse pressure is calculated as:

$$Pf = \gamma D \left(\frac{1}{8\sin\varphi} - 0.12\right) \quad (3)$$

The effect of cohesion and friction angle has also been studied by Liu [40] and the correlation equation with collapse pressure is given below,

$$Pf = \gamma D N\gamma - CNc \quad (4)$$

The angle of internal friction and the cohesion stability number was incorporated by Algha [35] as given in the below equation:

$$Nc = \frac{1.1}{\sin\varphi} - 0.5 \quad (5)$$

Combining Eqs. 2, 4 and 5, the empirical equation of support pressure having the effect of cohesion and angle of internal friction is given in Eq. 6. The equation is valid for soil conditions having cohesion not equal to zero and D<10m. Equation 6 is recommended for support pressure, considering both cohesion and angle of internal friction, particularly suitable for soil conditions with non-zero cohesion and tunnel diameters less than 10m. This equation helps to investigates the interrelationship between support pressure, cohesion, and internal friction within a specific geological context. This comprehensive examination provides the combined influence of these parameters on tunnel stability, enhancing the understanding of excavation risks in diverse geological settings.

$$Pf = \gamma D \left(\frac{1}{8\sin\varphi} - 0.12\right) - c\left(\frac{1.1}{\sin\varphi} - 0.5\right) \quad (6)$$

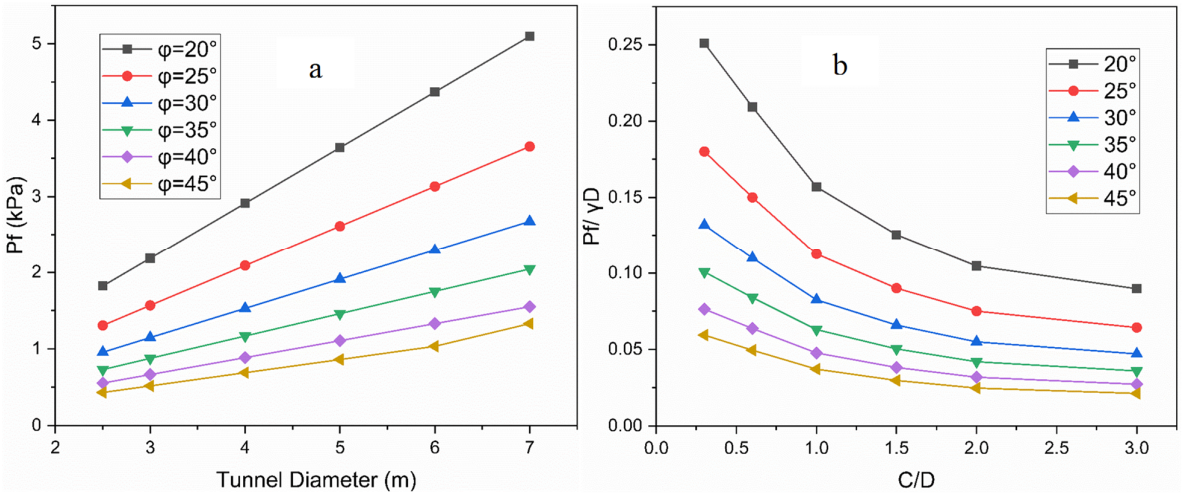

Figure 9. (a) Face support pressure and tunnel diameter and (b) the normalized face collapse pressure with C/D by incorporating friction angle

It was also reported in literature that [41] the face support pressure, at least up to the point of failure, is relatively unaffected by changes in the cover-to-diameter ratio (C/D). The cover-to-diameter ratio refers to the distance from the tunnel's outer surface to the surrounding ground, compared to the diameter of the tunnel [42]. Increasing the value of C/D decreases the $P_f/\gamma D$, (Figure 9b) and vice versa. This increase in face support pressure by decreasing C/D occurs due to the greater overlying rock mass exerting additional pressure on the tunnel face. It is often a critical parameter in tunnel design, particularly for assessing stability and ensuring safe excavation [43]. The linear relationship between the limiting support pressure and tunnel diameter is significant, as it provides a predictable and proportional increase in the required support pressure as the tunnel diameter increases [44]. The normalized face collapse pressure ($P_f/ \gamma D$) is representing as weighting coefficient (γN), which can also be referred as the soil stability number, shows that with increase in C/D its value decreased. But it was also noticed from Figure 10b that the angle of internal friction has a significant effect on soil stability number. For example, the collapse pressure value is the highest at C/D=0.5 for 20° angle of internal friction, while at 45° the collapse pressure is almost negligible. To take into account the effect of angle of internal friction into the weighting coefficient, Figure 10a is plotted using $N\gamma = \frac{1}{8sin\varphi} - 0.12$. It was observed that the weighting coefficient decreased sharply from 20° to 30° of angle of internal friction. The curve is then flat up to 45° angle of internal friction. Hence internal friction value greater than 45° indicated a little effect on weighting coefficient. The results from the experiments conducted suggest that the cover-to-diameter ratio (C/D) has minimal impact on the face support pressure at failure. Additionally, their results indicate that there is a linear relationship between the limiting support pressure and the tunnel diameter. This is an important understanding for tunneling, as it implies that the face support pressure, at least up to the point of failure, is relatively unaffected by changes in the cover-to-diameter ratio [34].

The observed minimal impact of the cover-to-diameter ratio (C/D) on face support pressure and the linear relationship between limiting support pressure and tunnel diameter highlight the strength of these parameters in tunnel design. This stability in face support pressure, irrespective of C/D changes, highlights the reliability of current design practices [16]. Moreover, the predictable increase in required support pressure with tunnel diameter growth, as revealed by the linear relationship, offers a practical tool for scalable and proportional design enhancing the efficiency and safety of tunnel excavation [45].

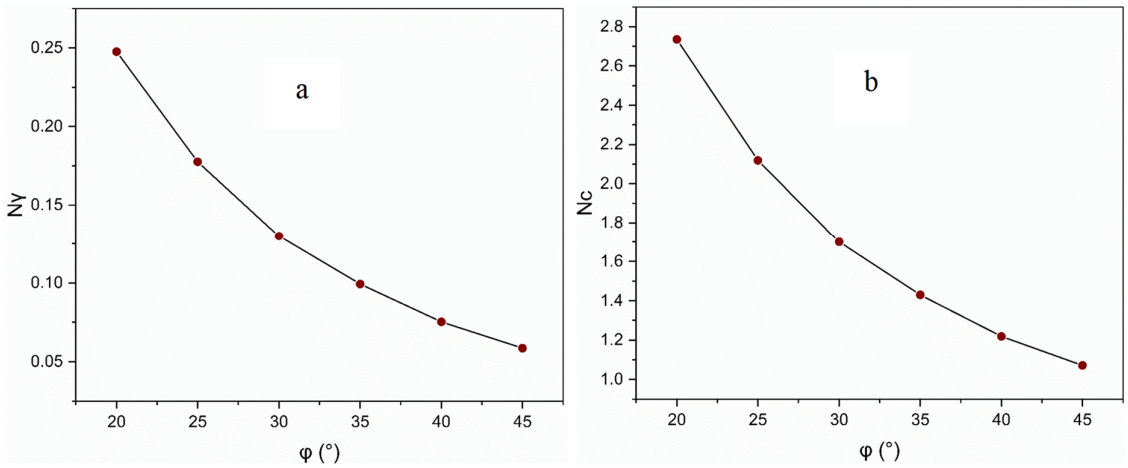

Figure 10 (a) Soil stability number and friction angle (b) Cohesion stability number and friction angle

In order to incorporate the effect of cohesion stability number N_c and friction angle Figure10b is plotted using the Eq. 7 [35]. It was noticed that the N_c shows a similar trend as Nγ. The N_c value decreased with increasing angle of internal friction.

$$Nc = \frac{1.1}{\sin\varphi} - 0.5 \quad (7)$$

An interesting observation is that the trend exhibited by N_c is similar to that of Nγ. Specifically, as the angle of internal friction increases, the value of N_c decreases. As the angle of internal friction rises, indicating a material's resistance to sliding or shearing, the value of N_c decreases. This indicates that an increase in the friction angle might lead to a reduction in the cohesion effect on stability [46]. It is essential to interpret this relationship carefully, as it could impact the overall stability of rock mass that rely on cohesion for support. The correlation of N_c and Nγ and angle of internal friction is given in Table 2. The decrease in N_c with a higher internal friction angle suggests that the material's increased resistance to sliding or shearing diminishes the effectiveness of cohesion in providing stability. This trend aligns with the understanding that higher internal friction implies a more self-supporting material. Additionally, this observation emphasizes the intricate balance required in tunneling and rock engineering projects, where the reliance on cohesion for support may be compromised in materials with elevated internal friction. Careful consideration of these relationships is important for accurate stability assessments and informed design decisions [45].

Table 2. The results of soil stability number and weight coefficient

Nc	Nγ	Pf, φ =20° KPa	Pf, φ =25° KPa	Pf, φ =30° KPa	Pf, φ =35° KPa	Pf, φ =40° KPa	Pf, φ =45° KPa
2.74	0.25	0.25	0.18	0.13	0.10	0.08	0.06
2.12	0.18	0.21	0.15	0.11	0.08	0.06	0.05
1.70	0.13	0.16	0.11	0.08	0.06	0.05	0.04
1.43	0.10	0.13	0.09	0.07	0.05	0.04	0.03
1.22	0.08	0.10	0.08	0.05	0.04	0.03	0.02
1.07	0.06	0.09	0.06	0.05	0.04	0.03	0.02

Figure11 shows the collapse pressure using the modified Eq. 6 after incorporating the effect of the cohesion and angle of internal friction (30°). It was observed that the collapse pressure decreased with increasing tunnel diameter. The results are given in Table 3. The decrease in collapse pressure with increasing tunnel diameter highlights the essential role of tunnel size. The incorporation of cohesion and an angle of internal friction (30°) in the modified equation reveals their significant impact on predicting collapse pressures, emphasizing the need for understanding geotechnical properties.

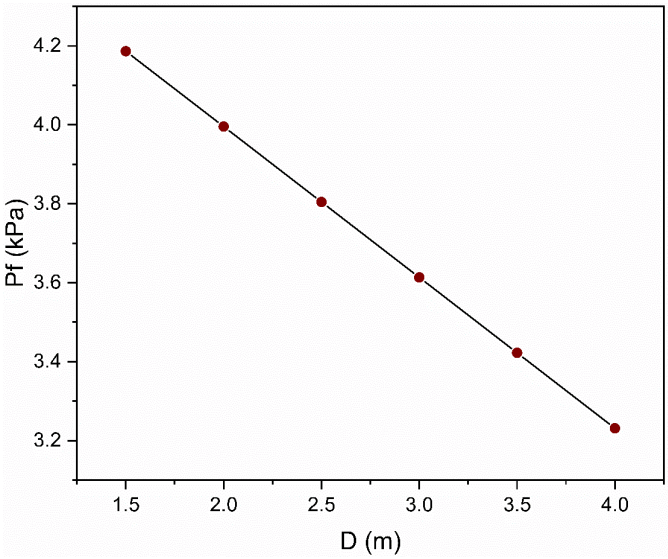

Figure 11. Collapse pressure and Tunnel diameter using the modified equation

Table 3. The results of collapse pressures for different empirical equations

D (m)	φ	C (MPa)	Pf Eq (3), KPa	Pf (Eq.4), KPa	P f (Eq.6), KPa	K
1.5			0.57	4.187	4	
2			0.76	3.996	4	
2.5	30°	2.8	0.96	3.805	4	3.28
3			1.15	3.613	4	
3.5			1.34	3.422	3	

6. Conclusions

This study revealed that stress redistribution surrounding the tunnel is restricted to a localized area, showing elastic behavior beyond a peak stress point. Isotropic in-situ stress conditions displayed a balanced stress distribution between tunnels. The incorporation of numerical modeling, coupled with an approximate method, strongly validated stress estimations, presenting a more precise depiction of the intricate rock mass. The following conclusions drawn from the numerical analysis further underscore the significance of these results:

- The study reveals that stress redistribution around the tunnel is concentrated within a 2-meter radius, with a peak stress point marking the shift from plastic to elastic behavior. This understanding is important for evaluating tunnel stability and long-term ground behavior.
- The isotropic in-situ stress conditions demonstrate a well-balanced stress distribution between the tunnels, validating stress estimations and providing specific information into the complex rock mass of the Himalayas.
- Dynamic stress changes during the excavation of the second tunnel led to immediate stress relief, activating secondary ground disturbances that gradually weaken the rock mass between the twin tunnels.
- The consistent strength factor of 1.3 for both single and twin tunnels reflect a reliable design approach, ensuring a safety margin against tensile failure. This uniformity implies a consistent level of tensile strength in the rock mass or material surrounding the tunnels.
- The increased angle of internal friction is observed to decrease the cohesion stability number, emphasizing the importance of considering both cohesion and friction in stability analyses and design processes.
- Stress accumulation near tunnel openings and the decline in the weighting coefficient between 20° and 30° of the angles of internal friction indicate a localized impact, with minimal influence on the far-field in-situ stress.
- The cover-to-diameter ratio (C/D) has minimal influence on face support pressure

at failure, establishing a linear relationship between the limiting support pressure and tunnel diameter.

References

[1]. Fu, J., Safaei, M.R., Haeri, H., et al. (2022) Experimental Investigation on Deformation Behavior of Circular Underground Opening in Hard Soil using a 3D Physical Model. *Journal of Mining and Environmen*t, *13*(3), 727-749.

[2]. Rezaei, A.S., Sarfarzi, V., Babanouri,N., Omidimanesh,M., Jahanmiri, S., (2023). Failure Mechanism of Rock Pillar Containing Two Edge Notches: Experimental Test and Numerical Simulation.

[3]. Wan, M., Standing, J.R., Potts, D.M., Burland, J.B., (2017). Measured short-term ground surface response to EPBM tunnelling in London Clay. *Géotechnique*, *67*(5), 420-445.

[4]. Luciani, A., and Peila, D., (2019). Tunnel Waterproofing: Available Technologies and Evaluation Through Risk Analysis. *International Journal of Civil Engineering*, *17*(1), 45-59.

[5]. Wang, X., Jinxinget, L., He, S., Garnes, R.S., Zhang, Y., (2020). Karst geology and mitigation measures for hazards during metro system construction in Wuhan, China. *Natural Hazards*, *103*(3), 2905-2927.

[6]. Gong, C., Ding, W., Xie, D., (2020). Twin EPB tunneling-induced deformation and assessment of a historical masonry building on Shanghai soft clay. *Tunnelling and Underground Space Technology*, 98, 103300.

[7]. Sarfarazi, V., (2020). Behavior of Tunnel and Neighboring Joint with and without Presence of Rock Bolt under biaxial loads; Particle Flow Code Approach. *Journal of Mining and Environment*, *11*(3), 855-864.

[8]. Doležalová, M.,(2001). Tunnel complex unloaded by a deep excavation. *Computers and Geotechnics*, 28(6-7), 469-493.

[9]. Sharma, J., Hefny, A.M.,Zhao, J., Chan, C.W., (2001). Effect of large excavation on deformation of adjacent MRT tunnels. *Tunnelling and Underground Space Technology*, *16*(2) 93-98.

[10]. Hu, Z., (2003). Design and construction of a deep excavation in soft soils adjacent to the Shanghai Metro tunnels. *Canadian Geotechnical Journal*, *40*(5), 933-948.

[11]. Doležalová, M., (2001). Tunnel complex unloaded by a deep excavation. *Computers and Geotechnics*, 28(6), 469-493.

[12]. Sharma, J.S., (2001). Effect of large excavation on deformation of adjacent MRT tunnels. *Tunnelling and Underground Space Technology*, *16*(2), 93-98.

[13]. Wang, W., Xu., Z. and Li., Q., (2018) Design and Construction of Deep Excavations in Shanghai. *Geotechnical Research*, 5, 1-55.

[14]. Sarfarazi, V., Asgari, K., Abad, S.M.B., (2021). Interaction between tunnel and surface foundation using PFC2D. *Journal of Mining and Environment, 12*(3), 785-798

[15]. Zhang, J.F., and Chen, J.J., (2013). Prediction of tunnel displacement induced by adjacent excavation in soft soil. *Tunnelling and Underground Space Technology*, 36, 24-33.

[16]. Athar, M.F., Zaid, M., Sadique, R., (2019). Stability of Different shapes of Tunnels in Weathering Stages of Basalt.

[17]. Luc Leroy, M., Ndop, J., Ndjaka, J., (2015). Numerical investigations of stresses and strains redistribution around the tunnel: Influence of transverse isotropic behavior of granitic rock, in situ stress and shape of tunnel. *Journal of Mining Science,* 51, 497-505.

[18]. Fama, M.E.D., 3 - Numerical Modeling of Yield Zones in Weak Rock, in Analysis and Design Methods, C. Fairhurst, Editor. 1993, Pergamon: Oxford. p. 49-75.

[19]. Kirsch, A.,(2010). Experimental investigation of the face stability of shallow tunnels in sand. *Acta Geotechnica,* 5, 43-62.

[20]. Hou, C., Zhong, J., Yang, X., (2023). Three-dimensional stability assessments of a non-circular tunnel face reinforced by bolts under seepage flow conditions. *Tunnelling and Underground Space Technology*, 131, 104831.

[21]. Ninić, J., (2020). Integrated parametric multi-level information and numerical modelling of mechanised tunnelling projects. *Advanced Engineering Informatics,* 43, 101011.

[22]. Guan, K., (2018). A finite strain numerical procedure for a circular tunnel in strain-softening rock mass with large deformation. International Journal of Rock Mechanics and Mining Sciences, 112, 266-280.

[23]. Hoek, E., Diederichs, M.S.,(2006). Empirical estimation of rock mass modulus. *International Journal of Rock Mechanics and Mining Sciences*, *43*(2), 203-215.

[24]. Shiau, J., Al-Asadi, F.,(2020). Three-dimensional heading stability of twin circular tunnels. *Geotechnical and Geological Engineering,* 38, 2973-2988.

[25]. Islam, M.S., Iskander, M.,(2023). Three-dimensional numerical investigation of ground settlement caused by piggyback twin tunnels. *Tunnelling and Underground Space Technology*, 134, 104970.

[26]. Najm, S.J., Daraei, A.,(2023). Forecasting and controlling two main failure mechanisms in the Middle East's longest highway tunnel. *Engineering Failure Analysis*, 146, 107091.

[27]. Chehade, F.H., Shahrour, I.,(2008). Numerical analysis of the interaction between twin-tunnels: Influence of the relative position and construction procedure. *Tunnelling and underground space technology*, *23*(2), 210-214.

[28]. Liu, Z., et al., (2021). A simplified two-stage method to estimate the settlement and bending moment of upper tunnel considering the interaction of undercrossing twin tunnels. *Transportation Geotechnics*, 29, 100558.

[29]. Zheng, G., et al., (2023). Relating twin-tunnelling-induced settlement to changes in the stiffness of soil. *Acta Geotechnica*, *18*(1), 469-482.

[30]. Abbas, N., et al.,(2022). Correlation of Schmidt Hammer Rebound Number and Point Load Index with Compressive Strength of Sedimentary, Igneous and Metamorphic Rocks. *Journal of Mining Science, 58*(6), 903-910.

[31]. Zeng, G., Wang, H. Jiang, M.,(2023). Analytical stress and displacement of twin noncircular tunnels in elastic semi-infinite ground. *Computers and Geotechnics,*160, 105520.

[32]. Shah, k.S., et al., (2023). Analysis of Granite Failure Modes and Energy Conversion Under Uniaxial Compression at Various Temperatures. *Journal of Mining and Environment*, *14*(2), 493-506.

[33]. Bobet, A., (2010). Numerical methods in geomechanics. *The Arabian Journal for Science and Engineering*, 35.

[34]. Barpi, F., and Peila, D., (2012). Influence of the tunnel shape on shotcrete lining stresses. *Computer-Aided Civil and Infrastructure Engineering*, *27*(4), 260-275.

[35]. Alagha, A.S.N., and Chapman, D.N., (2019). Numerical modelling of tunnel face stability in homogeneous and layered soft ground. *Tunnelling and Underground Space Technology*, 94, 103096.

[36]. Ye, Z., et al., (2023). A digital twin approach for tunnel construction safety early warning and management. *Computers in Industry*, 144, 103783.

[37]. Zhang, H., et al., (2023). Stability evaluation of rock pillar between twin tunnels using the YAI. *Scientific Reports*, 13(1), 13187.

[38]. Islam, M.S., and Iskander, M., (2021). Twin tunnelling induced ground settlements: A review. *Tunnelling and Underground Space Technology*, 110, 103614.

[39]. Leca, E., and Dormieux, L., (1990). Upper and lower bound solutions for the face stability of shallow circular tunnels in frictional material. *Géotechnique*, *40*(4), 581-606.

[40]. Liu, K., et al., (2021). Tunnel face stability in soils – Influence of the soil arching effect. *International Journal of Geomechanics*, 21.

[41]. Ads, A., Shariful Islam, M., Iskander, M., (2021). Effect of Face Losses and Cover-to-Diameter Ratio on Tunneling Induced Settlements in Soft Clay, Using Transparent Soil Models. *Geotechnical and Geological Engineering*, 39(8), 5529-5547.

[42]. Minh, N.V., (2016). Reducing the cover-to-diameter ratio for shallow tunnels in soft soils.

[43]. Lai, F., et al., (2021). Ground movements induced by installation of twin large diameter deeply-buried caissons: 3D numerical modeling. *Acta Geotechnica*, 16, 2933-2961.

[44]. Chortis, F., and Kavvadas, M., (2021). Three-dimensional numerical investigation of the interaction between twin tunnels. *Geotechnical and Geological Engineering*, *39*(8), 5559-5585.

[45]. Abbas, N., et al., (2023). Empirical Evaluation of RMR, GSI, and Q for Underground Excavations. *Iranian Journal of Science and Technology, Transactions of Civil Engineering*.

[46]. Bahri, M., et al., (2022). Numerical Model Validation for Detection of Surface Displacements over Twin Tunnels from Metro Line 1 in the Historical Area of Seville (Spain). *Symmetry*, *14*(6), 1263.

بررسی رفتار زمین در حفاری‌های زیرزمینی تحت شرایط تنش فشرده

نعیم عباس[۱،۲*] و که گنگ لی[۱]

۱ .دانشکده مهندسی منابع زمین، دانشگاه علم و فناوری کونمینگ، یونان، چین
۲. گروه مهندسی معدن دانشگاه بین المللی قراقورام (KIU)، گیلگیت، پاکستان

ارسال ۲۰۲۴/۰۲/۱۵، پذیرش ۲۰۲۴/۰۴/۱۰

* نویسنده مسئول مکاتبات: naeem.abbas@kiu.edu.pk

چکیده:

این مطالعه تأثیر پیوستگی، زاویه اصطکاک و قطر تونل را بر پایداری در چارچوب‌های مهندسی و ژئوتکنیکی بررسی کرد، در حالی که پیامدهای حفاری‌های مجاور را بر ارزیابی پایداری کلی در نظر گرفت. نتایج نشان می‌دهد که زاویه اصطکاک داخلی بالاتر منجر به کاهش عدد پایداری خاک و ضریب وزنی آن می‌شود. قطر تونل به طور قابل توجهی بر فشار تکیه گاه صورت تأثیر می‌گذارد، به طوری که قطرهای بزرگتر به دلیل افزایش تنش نیاز به تکیه گاه قوی تری دارند. زوایای اصطکاک بالاتر به تثبیت سطوح تونل و کاهش اثرات فشار مربوط به قطر کمک می‌کند. توزیع مجدد تنش در اطراف تونل در فاصله ۲ متری از مرکز قابل توجه است و در جاهای دیگر به رفتار الاستیک تبدیل می‌شود. ضریب ایمنی ۱.۳ جلوگیری از شکست کششی در تونل‌های تک و دوقلو را تضمین می‌کند. توزیع تنش متعادل بین تونل‌ها با تفاوت جزئی تحت تنش درجا همسانگرد مشاهده می‌شود. مدل‌سازی عددی تخمین تنش را افزایش می‌دهد و تغییرات را در حین حفاری تونل نشان می‌دهد و توده سنگ را ضعیف می‌کند. تجزیه و تحلیل منحنی واکنش زمین با اقدامات پشتیبانی، کاهش همگرایی تونل را پس از اجرا نشان می‌دهد، که استراتژی های پشتیبانی مانند پیچ های توسعه یافته با استفاده از رتبه بندی توده سنگ به روز شده را پیشنهاد می‌کند. این مطالعه طراحی تونل و ارزیابی پایداری را با درک جامع توزیع مجدد استرس و استراتژی‌های پشتیبانی بهبود می‌بخشد.

کلمات کلیدی: منحنی واکنش زمین، مدلسازی عددی، فشار پشتیبان، تونل سازی.